Novel Strains of *Culex Flavivirus* and Hubei Chryso-Like Virus 1 From the *Anopheles Costai* in Western Kenya

Olivia Wesula Lwande (✉ olivia.lwande@umu.se)
Department of Clinical Microbiology, Virology, Umeå University, Umeå https://orcid.org/0000-0002-9088-5388

Jonas Näslund
Swedish Defence Research Agency: Totalforsvarets Forskningsinstitut

Andreas Sjödin
Swedish Defence Research Agency: Totalforsvarets Forskningsinstitut

Rebecca Lantto
Department of Clinical Microbiology, Umeå University

Verah Nafula Luande
Department of Clinical Microbiology, Umeå University

Göran Bucht
Department of Clinical Microbiology, Umeå University

Clas Ahlm
Department of Clinical Microbiology, Umeå University

Bernard Agwanda
Mammology Section, National Museums of Kenya

Vincent Obanda
Department of Research Permitting and Compliance Wildlife Research and Training Institute

Magnus Evander
Department of Clinical Microbiology, Umeå University

Research

Keywords: Culex flavivirus, Hubei chryso-like virus 1, insect-specific viruses, Next generation target enrichment protocol, Western Kenya

Posted Date: October 19th, 2021

DOI: https://doi.org/10.21203/rs.3.rs-965111/v1

Abstract

Background

The continued development of advanced molecular tools, for instance DNA barcoding for identification of species and improvements of sequencing technologies is something that we have utilized in our vector surveillance research in order to discover viruses, both novel and already known viruses.

Methods

Mosquitoes (n=251) were captured using BG sentinel traps in May and July 2019 in Busia County, western Kenya. The mosquitoes were homogenized and screened in pools of ten (10) for presence of mosquito-borne viruses using virus isolation, PCR, and sequencing methods.

Results

Nineteen (19) mosquitoes generated results that indicated presence of a flavivirus. Barcoding of those positive mosquitoes revealed *Aedes aegypti* (1), *Mansonia uniformis* (6), *Anopheles costai* (3), *Culex pipiens* (5), *Culex spp* (1), *Coquilletidia metallica* (2) and *Culex quinquefasciatus* (1). By using an NGS target enrichment protocol specific for viruses, known as the Twist Comprehensive Viral Research Panel (CVRP) (Twist Biosciences), complete genome sequences of two viruses were identified. One was the single-stranded RNA *Culex flavivirus,* encoding a polyprotein, and the other was double-stranded RNA Hubei chryso-like virus 1. Both viruses were found in the same *Anopheles costai* mosquito and the homogenate showed cytopathogenic effect in both Vero B4 and C6/36 cells. Phylogenetic analyses suggest that the *Culex flavivirus* was closely related to a *Culex flavivirus* isolated from Uganda in 2008. All four Hubei chryso-like virus 1 segments clustered closely to the virus strains isolated from *Culex australicus* in Australia in 2015.

Conclusions

The detection of both viruses in a single mosquito indicates coinfection. The study findings shift our focus not only to pathogenic mosquito-borne viruses, but also to insect-specific viruses and other novel viruses and their role in the virus transmission cycle.

Background

Pathogenic mosquito-borne viruses, especially those belonging to major families such as *Togaviridae* (e.g. chikungunya virus), *Flaviviridae* (e.g. dengue virus), *Phenuiviridae* (e.g. Rift Valley fever virus) have been widely explored due to their significance to public and veterinary health [1–6]. Further, the recent advancement of powerful molecular tools including the next generation sequencing (NGS) platforms/methods/machines and the development of highly specialized bioinformatic platforms, has provided means of studying mosquito virome through metagenomic analyses. This has resulted in the discovery of novel viruses, and many of those are insect-specific viruses (ISVs), which belong to similar

families as their pathogenic counterparts [7–10]. Metagenomic analysis of virus sequences from mosquitoes has also revealed the presence of novel double stranded (ds) RNA viruses for example *Chrysoviridae* related (Hubei chryso-like virus 1), *Culex* Negev-like virus 3 (Biggie/Goutanap virus like) and virus related to Hubei reo-like virus 7 [11]. To our knowledge, the role of these viruses has not yet been established.

Since the discovery of the first ISVs (Cell-fusing agent virus - CFAV) about four decades ago [12], they have attracted attention in the last decade, due to their potential role in biocontrol, vaccine development and contribution towards the understanding of the mechanisms of host restriction and host range, as many of them do not infect vertebrate cells [13]. In terms of evolution, ISVs are believed to have developed long-ago with different lineages across diverse insect hosts mainly mosquitoes [14]. This is supported by vertical transmission studies where indications of possible integration of the virus genome into the vector's genome has been observed [15–17].

Most ISVs belong to the family *Flaviviridae*, for example: CFAV, which was initially isolated from an *A. aegypti* cell line supernatant inoculated onto an *Ae. albopictus* cell line; *Culex flavivirus* (CxFV) originally isolated from *Cx. pipiens* and other *Culex* spp. in 2007 in Japan [18] with subsequent isolations in in Guatemala, [19], Mexico [20, 21], the United States [22–26], Trinidad [25], Italy [15], Uganda [27], Europe [28, 29], China [30, 31], Brazil [32], Taiwan [33] and Argentina [34]; Kamiti River virus (KRV) isolated from the development stages of *Ae. mcintoshi* in 1999 in Kenya [35] and the Aedes flavivirus (AeFV) isolated from pools of *Ae. albopictus* and *Ae. flavopictus* in 2009 in Japan [36] with subsequent isolations in Europe [37] and the Americas [38, 39]. However, ISVs belonging to other virus families have also been discovered including: the *Reoviridae* family comprising of *Aedes pseudoscutellaris reovirus* (APRV) [40] and Fako virus (FAKV) [41]; *Togaviridae* comprising of Eilat virus isolated from *Anopheles coustani* in Israel in 1982-1984 [42] and *Peribunyaviridae* comprising of Badu virus isolated from *Culex* spp. mosquitoes in 2003 in Australia [43]. In addition to the new virus taxon- *Negevirus* which includes six prototype ISVs i.e. Negev (NEGV), Ngewotan (NWTV), Piura (PIUV), Loreto (LORV), Dezidougou (DEZV) and Santana (SANV), isolated from mosquitoes and phlebotomine sand flies collected in Brazil, Peru, USA, Ivory Coast, Israel and Indonesia [44]. The first ISV that was discovered in Kenya - the KRV [35], has been followed by other ISVs, for example CxFV from *Culex quinquefasciatus* in western and coastal regions of Kenya [45], *Aedes flaviviruses* from *Aedes aegypti*, *Aedes luteocephalus*, *Aedes* spp. and *Cx. pipiens* at Lake Victoria and *Anopheles flavivirus* from *An. gambiae* at Lake Baringo [46]. In addition, metagenomic analysis of Culex mosquitoes in Kwale, Kenya reveal the presence of diverse ISVs belonging to *Baculoviridae* [47].

The current study employed an NGS target enrichment protocol specific for viruses known as the Twist Comprehensive Viral Research Panel (CVRP) (Twist Biosciences) that covers reference sequences for 3,153 viruses, including 15,488 different strains. Although the method has not been applied on mosquito-borne viruses, it has been proven to be simple, reliable and accurate in screening of patient samples for infectious viral pathogens as in the case of respiratory viral co-infections with Rhino and Influenza virus

in patients confirmed to have SARS-CoV-2 [48]. The CVRP, has been designed to be applicable within the Illumina TruSeq RNA Library Prep for Enrichment and TruSeq RNA Enrichment workflows.

We tested whether the kit could be used to detect known and unknown viruses from mosquitoes. Therefore, we utilized the opportunity by testing randomly selected RNA extracted from mosquito samples obtained during an ongoing surveillance in western Kenya. We believe that the findings from this study may play a critical role in the discovery and detection of pathogens in vectors and hosts. Viral detection is critical to understanding the dynamics of viral populations and their interactions with vectors and hosts. This will enhance knowledge about unknown pathogens with potential to become emerging diseases in the future.

Methods

Study area

The study was conducted in Busia County, western Kenya close to the Kenya-Uganda border (figure 1). The region has a porous border system with no travel restrictions and most of the time people and goods are transported between Kenya and Uganda mainly by means of boats across Lake Victoria. The adjacent areas are heavily forested with bushy woodland which is infested with mosquitoes and tsetse flies. The population residing in this county includes both Luhya and Luo ethnic groups, as well as migrants from Uganda. The area is prone to flooding especially during long rainy seasons and this mainly occurs along the Budalangi flood plain area [49, 50].

Mosquito sampling and sorting

Two hundred and fifty-one (251) mosquitoes were captured in Funyula and Budalangi during May and July 2019. The mosquitoes were captured using the BG sentinel traps (Biogent, Germany). Mosquitoes were sorted based on date of collection, site and stored at -80°C, pending processing.

Mosquito homogenization

Each mosquito was prepared individually in a 2 mL micro tube with cap (Sarstedt, Nümbrecht, Germany) containing three 2 mm steel beads (AB Nino Lab, Upplands Väsby, Sweden) and 350 µL of 1x sterile filtered Dulbecco's Modified Eagles Media (DMEM) (Sigma-Aldrich, St Louis, MO, US) with 2% HEPES (Fisher Scientific, Fair Lawn, NJ, US). Homogenisation was performed using FastPreps 120 (Q-BIOgene, Irvine, CA, US) at 6.5 m/s for 20 s. The complete process was performed at 4°C to maintain the integrity of samples and virus viability, and subsequently stored at -80°C.

Pooling of homogenized individual mosquitoes

Sixty (60) µL of mosquito homogenate from 10 individual samples were used to create 10x pools, accordingly, adding up to a total volume of 600 µL. The complete process was performed at 4°C to maintain the integrity of samples and virus viability, and subsequently stored at -80°C.

Cell culture of mosquito pools

Vero B4 cells and C6/36 cells were grown in a 24 well plate to 80% confluency in DMEM and Leibovitz media containing 10% fetal bovine serum (FBS) (GE Healthcare Life Sciences, South Logan, UT, US) and 2% penicillin/streptomycin (PEST) (GE Healthcare Life Sciences, South Logan, UT, US) respectively. The cells were then rinsed with sterile phosphate-buffered saline (PBS), and 100 µL of clarified 10x mosquito homogenate was added to each well (in duplicate), followed by incubation at 37°C (Vero B4 cells) and 28°C (C6/36 cells) for 45 min to allow virus adsorption. After incubation, 1 mL DMEM and Leibovitz media supplemented with 2% fetal bovine serum (FBS) (GE Healthcare Life Sciences, South Logan, UT, US) and 2% penicillin, streptomycin (PEST) (GE Healthcare Life Sciences, South Logan, UT, US) was added into the wells and the cells allowed to incubate at 37°C (Vero B4 cells) and 28°C (C6/36 cells) for 14 days while observing cytopathogenic effect (CPE) on a daily basis. The supernatants of Vero B4 and C6/36 cells exhibiting CPE of approximately 50% were harvested from the wells by gently scraping the bottom of each well with a Pasteur pipette and transferred to 1 mL cryovials for storage at -80°C before a further round of inoculation, as previously described.

RNA extraction

Extraction of viral RNA, from the pooled and individual mosquito homogenates was performed with QIAmp® Viral RNA Mini Kit (QIAGEN, Hilden, Germany), According to the manufacturer's protocol (Spin Protocol). One hundred forty (140) µL of each CPE positive 10x mosquito homogenate pool was used as a sample volume and eluted in a final volume of 60 µL, collected in 1.5 mL sterile Eppendorf tubes and stored at -80°C.

cDNA synthesis, PCR, gel electrophoresis and sequencing

The extracted RNA was converted to cDNA using the Revert Aid RT kit (Thermo Fisher Scientific,Waltham, Massachusetts, US) according to manufacturer's instructions. PCR was performed using genus specific primers targeting the non-structural protein 5 (NS5) of the Flavivirus genome [51]. Briefly, conventional PCR was performed using the Phusion Green Hot Start II High-Fidelity PCR Master Mix (Thermo Fisher Scientific). For each reaction, 2 µL of template was used together with 10 µL of the 2x Phusion mix, 1.25 µL of both forward (FU 1; 5'- TAC AAC ATG ATG GGA AAG AGA GAG AA-3') and reverse primers (CFD2; 5'- GTG TCC CAG CCG GCG GTG TCA TCA GC-3') (10 pmol), 0.6 µL of DMSO and 4.9 µL of nuclease free water, up to a total reaction volume of 20 µL. Conditions for reactions were 98°C for 30 s for initial denaturation. Further, amplification was performed using 35 cycles of: 98°C for 7 s, 60°C for 15 s and 72°C for 20 s. Final extension was performed at 72°C for 7 min. The PCR products were analysed by gel electrophoresis using 3% agarose in 1x TAE with GelRed (Biotium Inc. Hayward, CA, US) and later purified with ExoSAP-IT kit (Thermo Fisher Scientific) and sent to Eurofin Genomics (Germany) for Sanger sequencing. Sequences were then aligned to previously identified Flavivirus strains in GenBank using the

Basic Local Alignment Search Tool (BLAST) provided by the National Center for Biotechnology Information.

DNA barcoding of mosquito species

Approximately 50 µL of the individual Flavivirus positive mosquito homogenates were used for DNA extraction using NucleoSpin® DNA Insect (Macherey-Nagel, Düren, Germany) according to the manufacturer's instructions. The DNA was stored at -80°C. Amplification of extracted DNA was performed using Phusion Green Hot Start II High-Fidelity PCR Master Mix (Thermo Fisher Scientific,) with a LCO/HCO primer pair, targeting the mitochondrial cytochrome c oxidase subunit I gene (COI) [52]. For each reaction, 2 µL of template was used together with 10 µL of 2x Phusion mix, 1.25 µL of both forward and reverse primers (10 pmol), 0.6 µL of DMSO and 4.9 µL of nuclease free water, up to a total reaction volume of 20 µL. Conditions for reactions were 98°C for 30 s for initial denaturation. Further, amplification was performed using 35 cycles of: 98°C for 7 s, 50°C for 15 s and 72°C for 20 s. Final extension was performed at 72°C for 7 min. PCR product was analysed by gel electrophoresis using 1.2% agarose in 1x TAE with GelRed (Biotium Inc. Hayward, CA, US) and later purified with ExoSAP-IT kit (Thermo Fisher Scientific,) and sent to Eurofin Genomics (Germany) for Sanger sequencing. Sequences were then aligned to previously identified mosquito species in GenBank using the Basic Local Alignment Search Tool (BLAST) provided by National Centre for Biotechnology Information.

Pan-Viral panel protocol

The RNA was converted to cDNA using ProtoScript II First Strand cDNA Synthesis Kit (E6560S) and New England Biolab's Random Primer 6 (S1230S). The NEBNext Ultra II Non-Directional RNA Second Strand Synthesis kit (E6111S) was subsequently used to convert single-stranded cDNA to dsDNA. Illumina TruSeq-compatible libraries were then generated using the Twist Biosciences, San Francisco, CA, USA.with Enzymatic Fragmentation (PN 101059 and 100401) and Unique Dual Indices (UDI) (PN 101307). Libraries were ultimately generated at a viral titre of 91.3 ng/µL. Hybridization capture was performed using the Twist Comprehensive Viral Research Panel (PNs 103545, 103547, 103548) and the Twist Standard Target Enrichment workflow. Approximately 9.6ng/µL of library was used in each 16-hour hybridization capture reaction. Following enrichment, libraries were sequenced with 75 bp paired-end reads on the Illumina MiSeq platform, using a MiSeq Reagent v3 150-cycles kit.

Taxonomic classification of metagenomic reads

Generated sequence reads were initially depleted for potential host reads by mapping to human reference (GRCh37) and mosquito species (*Aedes aegypti* strain LVP_AGWG and *Culex quinquefasciatus* strain JHB). Remaining sequence reads were classified using Kaiju [53] to give a profile of potential virus species in enriched samples.

Virus genome assembly, coverage analysis and variant detection

Depleted sequence reads were assemblies using Megahit [54] and Trinity [55] and contigs longer than 1000bp were kept and polished using Pilon [56]. Remaining contigs were annotated using Prokka [57] and characterized using Checkv [58] and Virsorter [59]. Predicted virus sequences were then further annotated and confirmed using NCBI Blast.

Amino acid substitution and phylogenetic analyses

The sequences obtained from the study (accession numbers OK413943, OK413944 OK413945 OK413946 [Hubei chryso-like virus segment 1 to 4 respectively] and OK413947 [CxFV]) segments were aligned to the respective virus sequences using Muscle programme incorporated within MEGA6 [60]. Phylogenetic trees were constructed from nucleotide alignments using the Maximum Likelihood method based on the Tamura-Nei model [61]. Evolutionary analyses were conducted in MEGA6 [60].

Results

A total of 26 pools (10 mosquitoes/pool), were generated from the 251 mosquito homogenates. Five pools showed CPE, two had clear CPE in both C6/36 and VeroB4 cells, two with CPE only in C6/36 cells and one showed CPE only in Vero B4 cells. Of the 50 mosquitoes that constituted the five flavivirus positive pools, 19 were flavivirus positive by RT-PCR. Barcoding results of the 19 mosquitoes revealed seven different species, including, *Aedes aegypti* (1), *Mansonia uniformis* (6), *Anopheles costai* (3), *Culex pipiens* (5), *Culex spp* (1), *Coquilletidia metallica* (2) and *Culex quinquefasciatus* (1). We had resources to investigate 5 of the 19 mosquitoes with the Twist pan-viral hybrid-capture panel and we selected mosquito homogenates that showed CPE in both C6/36 and VeroB4 cells.

One of the five individual mosquitoes subjected to the Twist CVRP hybrid-capture yielded two complete virus genome sequences. One was a CxFV encoding a polyprotein, and the other was four complete segments of the double stranded RNA virus Hubei chryso-like virus 1. Barcoding results indicated that both viruses were isolated from the same *Anopheles costai* mosquito.

Phylogenetic analysis of the detected CxFV indicated that it was closely related to the Ugandan strain isolated from *Cx. quinquefasciatus* in Uganda in 2008 (figure 2). All the Hubei chryso-like virus 1 segments clustered evenly with their respective virus segments from similar viruses detected in *Cx. australicus* and *Cx. globocoxitus* from Australia in 2015 (figures 3, 4, 5 and 6). The *An. costai* mosquito clustered together with *An. costai* from Colombia (figure 7).

Discussion

The study findings revealed the presence of two different viruses, CxFV and Hubei Chryso-like virus 1 from an individual *An. costai* mosquito, sampled in western Kenya. The findings implied that *Anopheles* mosquitoes may play a role in the transmission and maintenance of CxFV in nature. The role of other mosquito species in the transmission of CxFV and other insect specific viruses should be explored considering their possible role as biological control agents and serve as a basis for arbovirus protein

expression through generation of ISVs/Arbovirus chimeras. The findings may provide insights to a whole new knowledge in the ISVs-mosquito interaction as we hypothesize that ISVs may not be mosquito-specie specific. For example, despite the detection of CxFV from a majority of studies, the virus was initially detected *An. sinensis* in China [62] and lately in *An. costai* in western Kenya.

The detection of Hubei chryso-like virus highlighted the ability of mosquitoes to carry viruses which remain taxonomically unclassified and may have an influence on the mosquito vector competence. There is paucity of data on actual classification of Hubei chryso-like virus. To date the virus belongs to the unclassified Riboviria, which comprises of unclassified RNA viruses. Hubei chryso-like virus is a double-stranded RNA virus, and the presence of both a single-stranded RNA virus (CxFV) and the dsRNA Hubei chryso-like virus in a single mosquito may have an influence on antiviral RNA interference [63–65]. Hubei chryso-like virus was originally detected in mosquitoes in China and the virus is detected in *Culex* mosquitoes in Australia [66, 67]. To our knowledge this is the first isolation of four complete segments of Hubei-Chryso-like virus in the *An. costai* as previous isolations have been made on *Culex* mosquitoes [68]. Interestingly, the *An.costai* mosquito was co-infected with CxFV and Hubei-Chryso-like virus. However, whether the co-infection of either viruses enhances or antagonizes vector competence of the infected mosquito needs to be investigated. Previous studies have pointed the ability of insect specific virus reducing the transmission potential of pathogenic viruses such as Chikungunya virus, Dengue virus, West Nile virus and Zika virus [17, 69, 70].

The study highlights the application and usefulness of CVRP in the discovery of ISVs. To our knowledge this is the first time the method has been utilised to detect viruses from mosquito samples. So far, the method has been deemed valid in screening of patient samples and asymptomatic health care personnel for SARS-CoV-2 [71, 72]. The fact that the method was able to achieve sequence of the entire CxFV genome and all four segments of the Hubei chryso-like virus 1 demonstrates its efficiency and robustness. Therefore, we believe that the TPVP offers a platform that could help in solving challenges emanating from the inability to detect unknown viral pathogens.

Through the use of Twist CVRP hybrid-capture, full genome sequences of CxFV and Hubei chryso-like virus 1 from an *An. costai* mosquito have been generated.

Conclusions

The findings implied that Twist CVRP hybrid-capture may be a robust method that could be applied for the direct detection of ISVs and other viruses vectored by mosquitoes. Moreover, the findings contributed to the much-needed genetic data, especially for the unclassified dsRNA viruses like Hubei chryso-like virus 1 which is deficient at the moment.

Abbreviations

AeFV Aedes flavivirus

APRV *Aedes pseudoscutellaris reovirus*

BLAST Basic Local Alignment Search Tool

CFA Cell-fusing agent virus

CPE Cytopathogenic effect

CVRP Twist Comprehensive Viral Research Panel

CxFV Culex flavivirus

DEZV Dezidougou

DMEM Dulbecco's Modified Eagles Media

FAKV Fako virus

FBS Fetal bovine serum

KRV Kamiti River virus

ISVs Insect-specific viruses

LORV Loreto

NEGV Negev

NGS Next generation sequencing

NWTV Ngewotan

PEST Penicillin/streptomycin

PIUV Piura

SANV Santana

Declarations

Ethics approval and consent to participate

Not applicable

Consent for publication

Not applicable

Availability of data and materials

The datasets supporting the conclusions regarding sequences in this article will be available in GenBank (https://www.ncbi.nlm.nih.gov/genbank/) with accession numbers OK413943- OK413947.

Competing interests

The authors declare no competing interests.

Funding

The project was supported by the Swedish Research Council grant 2017-05607 (Magnus Evander).

Authors' contributions

ME, CA, OWL, JN, GB, BA, VO conceived the project, VO, BA did the fieldwork, OWL, RL, VNL did the lab work, JN, AS and OWL performed sequencing and phylogenetic analysis, OWL, JN, AS, GB analysed data, ME, OWL, CA sketched the draft manuscript and all authors read and approved the final manuscript.

Acknowledgments

Mosquito sampling team in Kenya. Emelie Näslund Salomonsson, and Stina Bäckman for their support during sequencing.

References

1. Zeller H, et al., *Mosquito-borne disease surveillance by the European Centre for Disease Prevention and Control.* 2013. **19**(8): p. 693-698.
2. Hassan OA, et al., *The 2007 rift valley fever outbreak in Sudan*. 2011. 5(9): p. e1229.
3. Baudin M, et al., *Association of Rift Valley fever virus infection with miscarriage in Sudanese women: a cross-sectional study*. 2016. 4(11): p. e864-e871.
4. Powers AM, C.H.J.J.o.G V, Logue. *Changing patterns of chikungunya virus: re-emergence of a zoonotic arbovirus*. 2007. 88(9): p. 2363–2377.
5. Sang R. and L.J.E.A.m.j. Dunster. The growing threat of arbovirus transmission outbreaks in Kenya: a review. 2001;78(12):655–61.
6. Konongoi L, et al., *Detection of dengue virus serotypes 1, 2 and 3 in selected regions of Kenya: 2011–2014.* 2016. **13**(1): p. 182.
7. Roundy CM, et al. Insect-Specific Viruses: A Historical Overview and Recent Developments. Adv Virus Res. 2017;98:119–46.
8. Shi M, et al. Redefining the invertebrate RNA virosphere. 2016;540(7634):539–43.
9. Junglen S, C.J.C.O.i M, Drosten. Virus discovery recent insights into virus diversity in arthropods. 2013;16(4):507–13.

10. Frey KG, et al., *Bioinformatic characterization of mosquito viromes within the Eastern United States and Puerto Rico: discovery of novel viruses*. 2016. 12: p. EBO. S38518.
11. Vibin J, et al., *Metagenomics detection and characterisation of viruses in faecal samples from Australian wild birds*. 2018. 8(1): p. 1–23.
12. Stollar V, Thomas VLJV. *An agent in the Aedes aegypti cell line (Peleg) which causes fusion of Aedes albopictus cells*. 1975. 64(2): p. 367–377.
13. Roundy CM, et al., *Insect-specific viruses: a historical overview and recent developments*, in *Advances in Virus Research*. 2017, Elsevier. p. 119-146.
14. Cook S, et al., *Novel virus discovery and genome reconstruction from field RNA samples reveals highly divergent viruses in dipteran hosts*. 2013. 8(11): p. e80720.
15. Roiz D, et al., *Detection of novel insect flavivirus sequences integrated in Aedes albopictus (Diptera: Culicidae) in Northern Italy*. 2009. 6(1): p. 93.
16. Cook S, et al., *Isolation of a new strain of the flavivirus cell fusing agent virus in a natural mosquito population from Puerto Rico*. 2006. 87(4): p. 735–748.
17. Bolling BG, et al., *Transmission dynamics of an insect-specific flavivirus in a naturally infected Culex pipiens laboratory colony and effects of co-infection on vector competence for West Nile virus*. 2012. 427(2): p. 90–97.
18. Hoshino K, et al., *Genetic characterization of a new insect flavivirus isolated from Culex pipiens mosquito in Japan*. 2007. 359(2): p. 405–414.
19. Morales-Betoulle M, et al. Culex flavivirus isolates from mosquitoes in Guatemala. 2008;45(6):1187–90.
20. Farfan-Ale JA, et al., *Detection of RNA from a novel West Nile-like virus and high prevalence of an insect-specific flavivirus in mosquitoes in the Yucatan Peninsula of Mexico.* 2009. **80**(1): p. 85-95.
21. Saiyasombat R, et al., *Isolation and sequence analysis of Culex flavivirus from Culex interrogator and Culex quinquefasciatus in the Yucatan Peninsula of Mexico*. 2010. 155(6): p. 983–986.
22. Blitvich BJ, et al., *Genomic sequence and phylogenetic analysis of Culex flavivirus, an insect-specific flavivirus, isolated from Culex pipiens (Diptera: Culicidae) in Iowa*. 2009. 46(4): p. 934–941.
23. Bolling BG, et al., *Insect-specific flaviviruses from Culex mosquitoes in Colorado, with evidence of vertical transmission*. 2011. 85(1): p. 169–177.
24. Crockett RK, et al., *Culex flavivirus and West Nile virus in Culex quinquefasciatus populations in the southeastern United States*. 2012. 49(1): p. 165–174.
25. Kim DY, et al. Characterization of Culex Flavivirus (Flaviviridae) strains isolated from mosquitoes *in*. the United States Trinidad. 2009;386(1):154–9.
26. Newman CM, et al. Culex flavivirus and West Nile virus mosquito coinfection and positive ecological association in Chicago. United States. 2011;11(8):1099–105.
27. Cook S, et al., *Isolation of a novel species of flavivirus and a new strain of Culex flavivirus (Flaviviridae) from a natural mosquito population in Uganda.* 2009. **90**(Pt 11): p. 2669.

28. Calzolari M, et al., *Arboviral survey of mosquitoes in two northern Italian regions in 2007 and 2008*. 2010. 10(9): p. 875–884.
29. Vázquez A, et al., *Novel flaviviruses detected in different species of mosquitoes in Spain*. 2012. 12(3): p. 223–229.
30. Huanyu W, et al. Isolation and identification of a distinct strain of Culex Flavivirus from mosquitoes collected *in*. Mainland China. 2012;9(1):73.
31. Liang W, et al. Distribution and phylogenetic analysis of Culex flavivirus *in*. mosquitoes in China. 2015;160(9):2259–68.
32. Machado DC, et al. First identification of Culex flavivirus (Flaviviridae) in Brazil. Intervirology. 2012;55(6):475–83.
33. Chen YY, et al. First detection of the Africa/Caribbean/Latin American subtype of Culex flavivirus in Asian country, Taiwan. Comp Immunol Microbiol Infect Dis. 2013;36(4):387–96.
34. Goenaga S, et al. New strains of Culex flavivirus isolated in Argentina. J Med Entomol. 2014;51(4):900–6.
35. Sang R, et al., *Isolation of a new flavivirus related to cell fusing agent virus (CFAV) from field-collected flood-water Aedes mosquitoes sampled from a dambo in central Kenya*. 2003. 148(6): p. 1085–1093.
36. Hoshino K, et al. Isolation and characterization of a new insect flavivirus from Aedes albopictus and Aedes flavopictus mosquitoes in Japan. Virology. 2009;391(1):119–29.
37. Roiz D, et al. Detection of a new insect flavivirus and isolation of Aedes flavivirus in Northern Italy. Parasit Vectors. 2012;5:223.
38. Fernandes LN, et al. Detection of Culex flavivirus and Aedes flavivirus nucleotide sequences in mosquitoes from parks in the city of São Paulo, Brazil. Acta Trop. 2016;157:73–83.
39. Haddow AD, et al. First isolation of Aedes flavivirus in the Western Hemisphere and evidence of vertical transmission in the mosquito Aedes (Stegomyia) albopictus (Diptera: Culicidae). Virology. 2013;440(2):134–9.
40. Attoui H, et al. Expansion of family Reoviridae to include nine-segmented dsRNA viruses: isolation and characterization of a new virus designated Aedes pseudoscutellaris reovirus assigned to a proposed genus (Dinovernavirus). Virology. 2005;343(2):212–23.
41. Auguste AJ, et al. A newly isolated reovirus has the simplest genomic and structural organization of any reovirus. J Virol. 2015;89(1):676–87.
42. Samina I, et al. Isolation of viruses from mosquitoes of the Negev Israel. 1986;80(3):471–2.
43. van-den-Hurk AF, et al. Domestic pigs and Japanese encephalitis virus infection, Australia. Emerg Infect Dis. 2008;14(11):1736–8.
44. Vasilakis N, et al., *Negevirus: a proposed new taxon of insect-specific viruses with wide geographic distribution*. 2013. 87(5): p. 2475–2488.

45. Iwashita H, et al. Mosquito arbovirus survey in selected areas of Kenya: detection of insect-specific virus. Trop Med Health. 2018;46:19.
46. Ajamma YU, et al., *Vertical transmission of naturally occurring Bunyamwera and insect-specific flavivirus infections in mosquitoes from islands and mainland shores of Lakes Victoria and Baringo in Kenya*. 2018. 12(11): p. e0006949.
47. Atoni E, et al. Metagenomic Virome Analysis of Culex Mosquitoes from Kenya and China. Viruses. 2018;10(1):30.
48. Kim KW, et al., *Respiratory viral co-infections among SARS-CoV-2 cases confirmed by virome capture sequencing.* 2020.
49. Mutiso FM. Integration of remote sensing (rs) and geographic information system (gis) in monitoring and management of floods; case study budalangi area. University of Nairobi; 2011.
50. Onywere SM, et al., *Assessing the challenge of settlement in Budalangi and Yala Swamp area in Western Kenya using Landsat Satellite Imagery.* 2011.
51. Bryant JE, et al. Isolation of arboviruses from mosquitoes collected in northern Vietnam. Am J Trop Med Hyg. 2005;73(2):470–3.
52. Folmer O, et al. DNA primers for amplification of mitochondrial cytochrome c oxidase subunit I from diverse metazoan invertebrates. Mol Mar Biol Biotechnol. 1994;3(5):294–9.
53. Menzel P, Ng KL, Krogh A. Fast and sensitive taxonomic classification for metagenomics with Kaiju. Nat Commun. 2016;7:11257.
54. Li D, et al. MEGAHIT: an ultra-fast single-node solution for large and complex metagenomics assembly via succinct de Bruijn graph. Bioinformatics. 2015;31(10):1674–6.
55. Grabherr MG, et al. Full-length transcriptome assembly from RNA-Seq data without a reference genome. Nat Biotechnol. 2011;29(7):644–52.
56. Walker BJ, et al. Pilon: an integrated tool for comprehensive microbial variant detection and genome assembly improvement. PLoS One. 2014;9(11):e112963.
57. Seemann T. Prokka: rapid prokaryotic genome annotation. Bioinformatics. 2014;30(14):2068–9.
58. Nayfach S, et al., *CheckV assesses the quality and completeness of metagenome-assembled viral genomes*. Nat Biotechnol, 2020.
59. Roux S, et al. VirSorter: mining viral signal from microbial genomic data. PeerJ. 2015;3:e985.
60. Tamura K, et al., *MEGA6: molecular evolutionary genetics analysis version 6.0*. 2013. 30(12): p. 2725–2729.
61. Tamura K, Nei MJMb, and evolution, *Estimation of the number of nucleotide substitutions in the control region of mitochondrial DNA in humans and chimpanzees.* 1993. **10**(3): p. 512-526.
62. Liang W, et al. Distribution and phylogenetic analysis of Culex flavivirus in mosquitoes in China. Arch Virol. 2015;160(9):2259–68.
63. McFarlane M, et al., *The Aedes aegypti Domino Ortholog p400 Regulates Antiviral Exogenous Small Interfering RNA Pathway Activity and ago-2 Expression*. mSphere, 2020. 5(2).

64. Keene KM, et al. RNA interference acts as a natural antiviral response to O'nyong-nyong virus (Alphavirus; Togaviridae) infection of Anopheles gambiae. Proc Natl Acad Sci U S A. 2004;101(49):17240–5.
65. Myles KM, et al., *Alphavirus-derived small RNAs modulate pathogenesis in disease vector mosquitoes*. 2008. 105(50): p. 19938–19943.
66. Williams SH, et al., *The Diversity and Distribution of Viruses Associated with Culex annulirostris Mosquitoes from the Kimberley Region of Western Australia*. Viruses, 2020. 12(7).
67. Shi M, et al., *High-Resolution Metatranscriptomics Reveals the Ecological Dynamics of Mosquito-Associated RNA Viruses in Western Australia*. J Virol, 2017. 91(17).
68. Shi M, et al., *High-resolution metatranscriptomics reveals the ecological dynamics of mosquito-associated RNA viruses in Western Australia*. 2017. 91(17).
69. Romo H, et al., *Restriction of Zika virus infection and transmission in Aedes aegypti mediated by an insect-specific flavivirus*. 2018. 7(1): p. 1–13.
70. Nasar F, et al., *Eilat virus induces both homologous and heterologous interference.* 2015. **484**: p. 51-58.
71. Lythgoe KA, et al., *SARS-CoV-2 within-host diversity and transmission.* 2021. **372**(6539).
72. Scaria V, *Asymptomatic reinfection in two healthcare workers from India with genetically distinct SARS-CoV-2.* 2020.

Figures

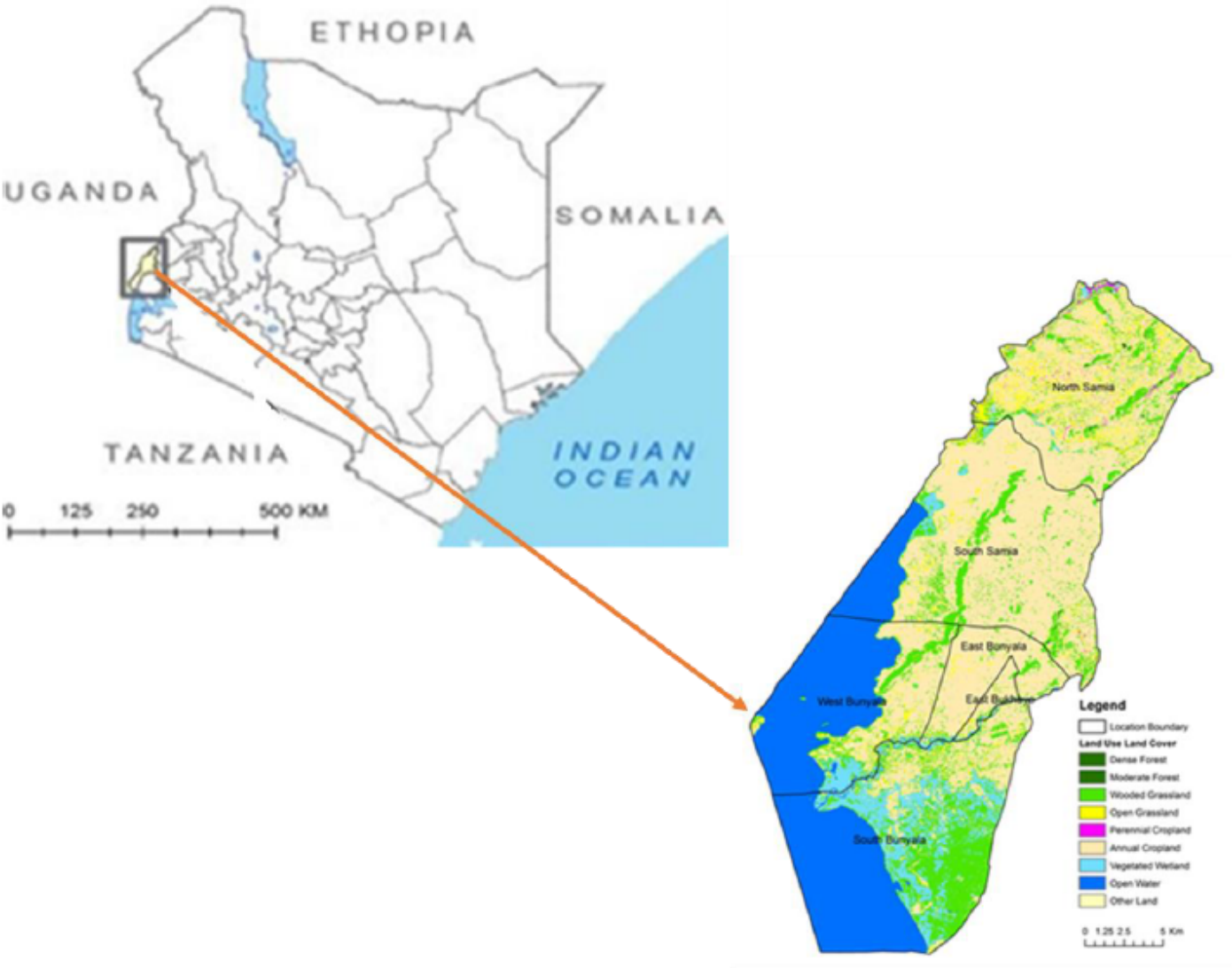

Figure 1

Map of Kenya showing study area in Busia County western Kenya.

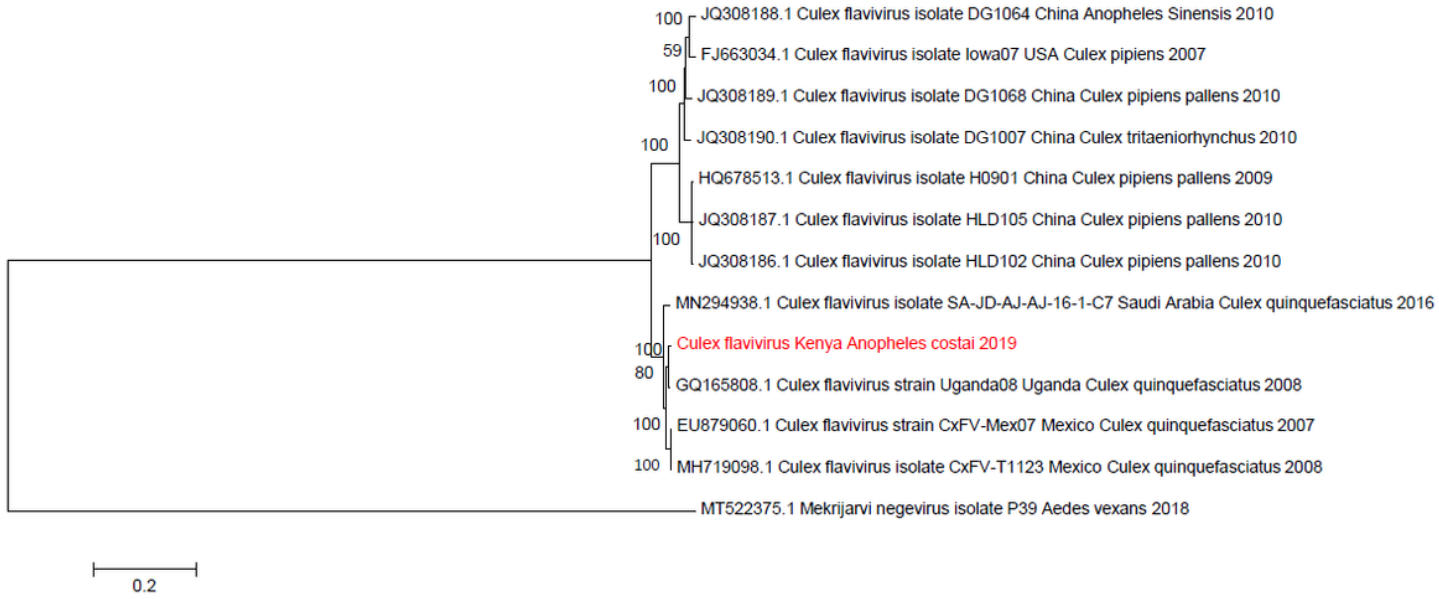

Figure 2

Phylogenetic analysis of complete genomes CxFV available in GenBank including the study isolate (in red). The evolutionary history was inferred by using the Maximum Likelihood method based on the Tamura-Nei model [61]. The tree with the highest log likelihood (-35607.4862) is shown. The percentage of trees in which the associated taxa clustered together is shown next to the branches. Initial tree(s) for the heuristic search were obtained by applying the Neighbor-Joining method to a matrix of pairwise distances estimated using the Maximum Composite Likelihood (MCL) approach. A discrete Gamma distribution was used to model evolutionary rate differences among sites (2 categories (+G, parameter = 0.8470)). The tree is drawn to scale, with branch lengths measured in the number of substitutions per site. The analysis involved 13 nucleotide sequences. Codon positions included were 1st+2nd+3rd+Noncoding. All positions containing gaps and missing data were eliminated. There were a total of 9434 positions in the final dataset. Evolutionary analyses were conducted in MEGA6 [60]. Mekrijarvi negevirus isolate P39 isolated from Ae. vexans in 2018 was used as an outgroup.

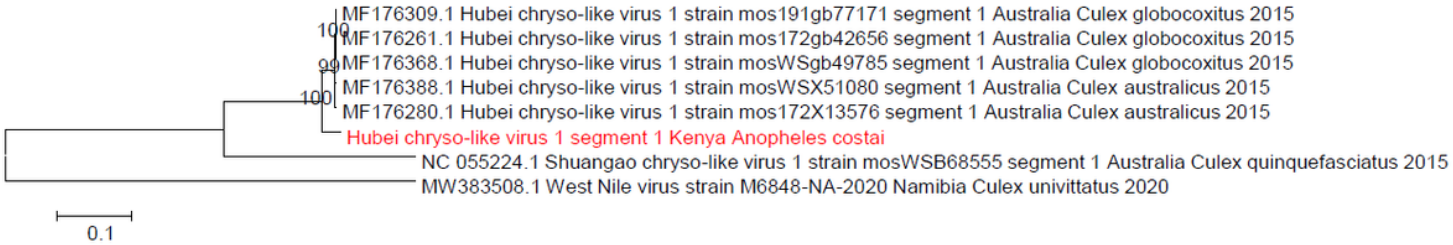

Figure 3

Phylogenetic analysis of complete genome segments of Hubei chryso-like virus 1 available in GenBank including the study isolate segments 1 (in red). Closely related virus - Shuangao chryso-like virus 1 strain mosWSB68555 segment 1 and West Nile virus strain M6848-NA-2020 as an outgroup. The evolutionary

history was inferred by using the Maximum Likelihood method based on the Tamura-Nei model [61].The tree with the highest log likelihood (-10489.0751) is shown. The percentage of trees in which the associated taxa clustered together is shown next to the branches. Initial tree(s) for the heuristic search were obtained by applying the Neighbor-Joining method to a matrix of pairwise distances estimated using the Maximum Composite Likelihood (MCL) approach. A discrete Gamma distribution was used to model evolutionary rate differences among sites (2 categories (+G, parameter = 1.9980)). The tree is drawn to scale, with branch lengths measured in the number of substitutions per site. The analysis involved 8 nucleotide sequences. Codon positions included were 1st+2nd+3rd+Noncoding. All positions containing gaps and missing data were eliminated. There were a total of 2888 positions in the final dataset. Evolutionary analyses were conducted in MEGA6 [60].

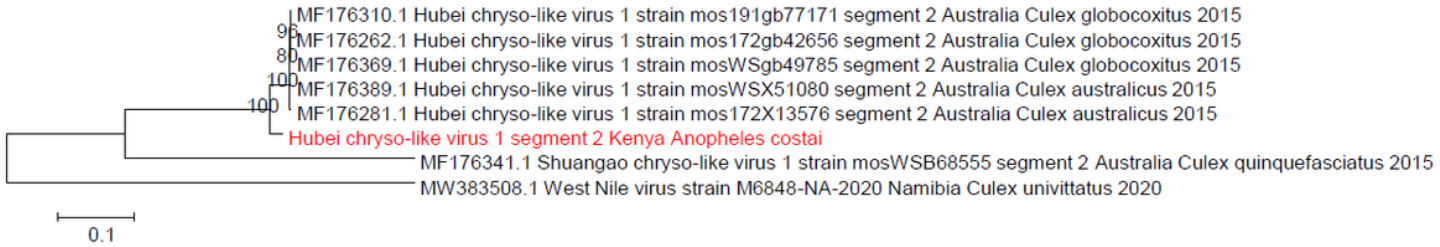

Figure 4

Phylogenetic analysis of complete genome segments of Hubei chryso-like virus 1 available in GenBank including the study isolate segments 2 (in red). Closely related virus - Shuangao chryso-like virus 1 strain mosWSB68555 segment 2 and West Nile virus strain M6848-NA-2020 as an outgroup. The evolutionary history was inferred by using the Maximum Likelihood method based on the Tamura-Nei model [61].The tree with the highest log likelihood (-9383.8153) is shown. The percentage of trees in which the associated taxa clustered together is shown next to the branches. Initial tree(s) for the heuristic search were obtained by applying the Neighbor-Joining method to a matrix of pairwise distances estimated using the Maximum Composite Likelihood (MCL) approach. A discrete Gamma distribution was used to model evolutionary rate differences among sites (2 categories (+G, parameter = 2.2850)). The tree is drawn to scale, with branch lengths measured in the number of substitutions per site. The analysis involved 8 nucleotide sequences. Codon positions included were 1st+2nd+3rd+Noncoding. All positions containing gaps and missing data were eliminated. There were a total of 2477 positions in the final dataset. Evolutionary analyses were conducted in MEGA6 [60].

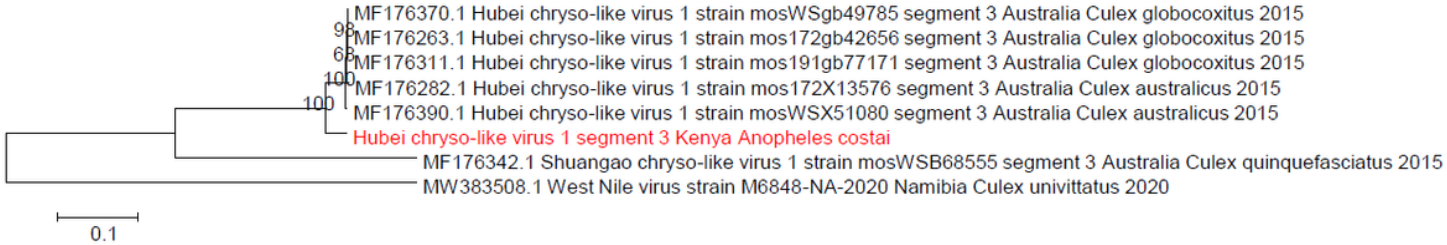

Figure 5

Phylogenetic analysis of complete genome segments of Hubei chryso-like virus 1 available in GenBank including the study isolate segments 3 (in red). Closely related virus - Shuangao chryso-like virus 1 strain mosWSB68555 segment 3 and West Nile virus strain M6848-NA-2020 as an outgroup. The evolutionary history was inferred by using the Maximum Likelihood method based on the Tamura-Nei model [61]. The tree with the highest log likelihood (-9826.3531) is shown. The percentage of trees in which the associated taxa clustered together is shown next to the branches. Initial tree(s) for the heuristic search were obtained by applying the Neighbor-Joining method to a matrix of pairwise distances estimated using the Maximum Composite Likelihood (MCL) approach. A discrete Gamma distribution was used to model evolutionary rate differences among sites (2 categories (+G, parameter = 1.7531)). The tree is drawn to scale, with branch lengths measured in the number of substitutions per site. The analysis involved 8 nucleotide sequences. Codon positions included were 1st+2nd+3rd+Noncoding. All positions containing gaps and missing data were eliminated. There were a total of 2610 positions in the final dataset. Evolutionary analyses were conducted in MEGA6 [60].

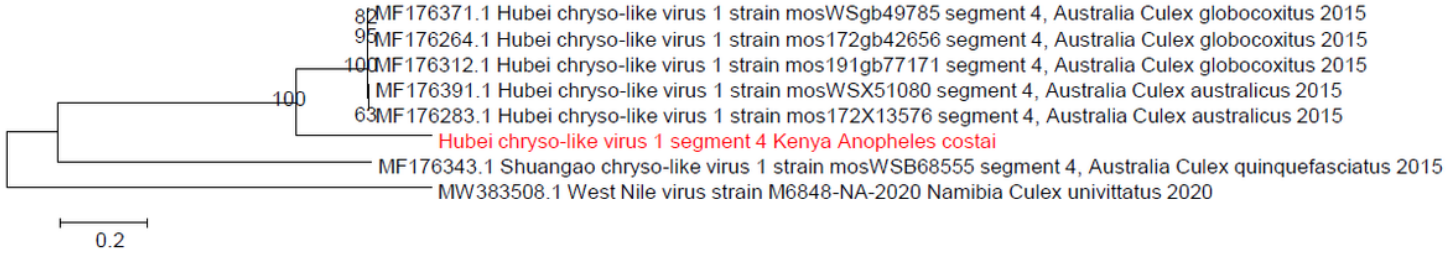

Figure 6

Phylogenetic analysis of complete genome segments of Hubei chryso-like virus 1 available in GenBank including the study isolate segments 4 (in red). Closely related virus - Shuangao chryso-like virus 1 strain mosWSB68555 segment 4 and West Nile virus strain M6848-NA-2020 as an outgroup. The evolutionary history was inferred by using the Maximum Likelihood method based on the Tamura-Nei model [61].The tree with the highest log likelihood (-14181.9308) is shown. The percentage of trees in which the associated taxa clustered together is shown next to the branches. Initial tree(s) for the heuristic search were obtained by applying the Neighbor-Joining method to a matrix of pairwise distances estimated using the Maximum Composite Likelihood (MCL) approach. A discrete Gamma distribution was used to model evolutionary rate differences among sites (2 categories (+G, parameter = 4.5239)). The tree is drawn to scale, with branch lengths measured in the number of substitutions per site. The analysis involved 8 nucleotide sequences. Codon positions included were 1st+2nd+3rd+Noncoding. All positions containing gaps and missing data were eliminated. There were a total of 2817 positions in the final dataset. Evolutionary analyses were conducted in MEGA6 [60].

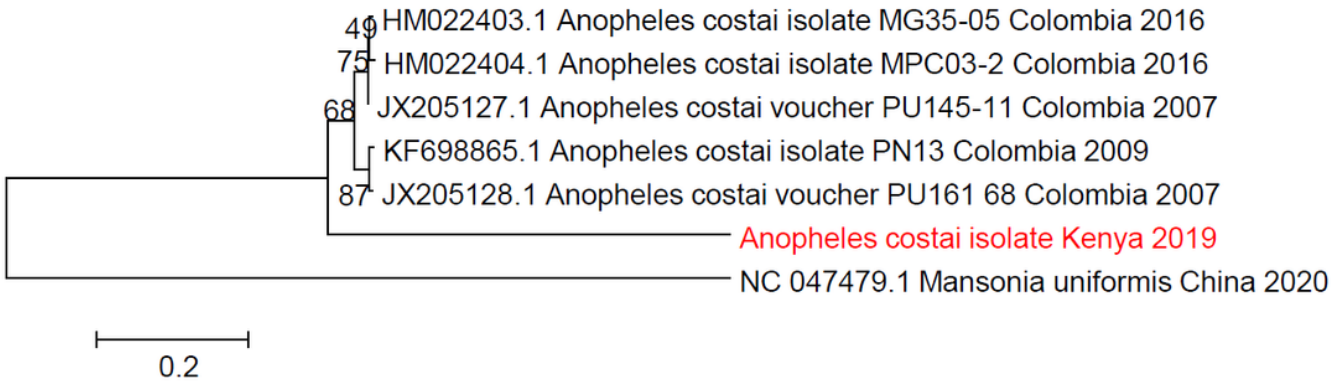

Figure 7

Phylogenetic analysis of cytochrome oxidase subunit 1 (COI) gene, partial cds; mitochondrial of An. costai (Colombia) including the study mosquito specie-An. costai (in red). The evolutionary history was inferred by using the Maximum Likelihood method based on the Tamura-Nei model [61]. The tree with the highest log likelihood (-1732.0365) is shown. The percentage of trees in which the associated taxa clustered together is shown next to the branches. Initial tree(s) for the heuristic search were obtained by applying the Neighbor-Joining method to a matrix of pairwise distances estimated using the Maximum Composite Likelihood (MCL) approach. A discrete Gamma distribution was used to model evolutionary rate differences among sites (2 categories (+G, parameter = 0.8474)). The tree is drawn to scale, with branch lengths measured in the number of substitutions per site. The analysis involved 7 nucleotide sequences. Codon positions included were 1st+2nd+3rd+Noncoding. All positions containing gaps and missing data were eliminated. There were a total of 475 positions in the final dataset. Evolutionary analyses were conducted in MEGA6 [60].